What is the potential of cropland albedo management in the fight against global warming? A case study based on the use of cover crops

Dominique Carrer, Gaétan Pique, Morgan Ferlicoq, Xavier Ceamanos, Eric Ceschia

What is the potential of cropland albedo management in the fight against global warming? A case study based on the use of cover crops

Environmental Research Letters

LETTER

OPEN ACCESS

RECEIVED
16 December 2017

REVISED
28 February 2018

ACCEPTED FOR PUBLICATION
13 March 2018

PUBLISHED
12 April 2018

What is the potential of cropland albedo management in the fight against global warming? A case study based on the use of cover crops

Dominique Carrer[1,4], Gaétan Pique[2,3], Morgan Ferlicoq[2], Xavier Ceamanos[1] and Eric Ceschia[2]

[1] CNRM UMR 3589, Météo-France/CNRS. 42, avenue Gaspard Coriolis, 31057 Toulouse Cedex, France
[2] CESBIO—Université Toulouse III/CNRS/CNES/IRD/INRA 18, avenue, Edouard Belin, bpi 2801, 31401 Toulouse Cedex 9, France
[3] ADEME, 20 avenue du Grésillé - BP 90406 49004 Angers Cedex 01, France
[4] Author to whom any correspondence should be addressed.

E-mail: dominique.carrer@meteo.fr

Keywords: surface albedo, radiative forcing, cropland, cover crops, agriculture

Abstract

Land cover management in agricultural areas is a powerful tool that could play a role in the mitigation of climate change and the counterbalance of global warming. First, we attempted to quantify the radiative forcing that would increase the surface albedo of croplands in Europe following the inclusion of cover crops during the fallow period. This is possible since the albedo of bare soil in many areas of Europe is lower than the albedo of vegetation. By using satellite data, we demonstrated that the introduction of cover crops into the crop rotation during the fallow period would increase the albedo over 4.17% of Europe's surface. According to our study, the effect resulting from this increase in the albedo of the croplands would be equivalent to a mitigation of 3.16 $MtCO_2$-eq.year^{-1} over a 100 year time horizon. This is equivalent to a mitigation potential per surface unit (m^2) of introduced cover crop over Europe of 15.91 gCO_2-eq.year^{-1}.m^{-2}. This value, obtained at the European scale, is consistent with previous estimates. We show that this mitigation potential could be increased by 27% if the cover crop is maintained for a longer period than 3 months and reduced by 28% in the case of no irrigation. In the second part of this work, based on recent studies estimating the impact of cover crops on soil carbon sequestration and the use of fertilizer, we added the albedo effect to those estimates, and we argued that, by considering areas favourable to their introduction, cover crops in Europe could mitigate human-induced agricultural greenhouse gas emissions by up to 7% per year, using 2011 as a reference. The impact of the albedo change per year would be between 10% and 13% of this total impact. The countries showing the greatest mitigation potentials are France, Bulgaria, Romania, and Germany.

1. Introduction

Today, the scientific community has evidence that the global warming issue (IPCC 2014) will not be resolved without clever solutions to reduce human-induced radiative forcing (RF). Possible strategies for climate mitigation include carbon dioxide removal (CDR) approaches or solar radiation management (SRM). While CDR aims at removing some CO_2 from the atmosphere, the goal of the latter approach is to counteract greenhouse gas-induced warming with an increase in the sunlight reflected back to space by an increased average albedo of the Earth. Lenton and Vaughan (2009) estimated that SRM strategies have the potential to cool the climate to its preindustrial state.

Various initiatives have been proposed to control the Earth's albedo. Although the dispersion of sulfate aerosols into the atmosphere is the most emblematic, this approach could have unintended and possibly harmful consequences (Robock *et al* 2009). Changing the surface albedo naturally seems to be a more appropriate solution. Some studies have suggested that an increase in surface albedo can be achieved by making roofs white worldwide (Akbari *et al* 2009, Jacobson and Hoeve 2011). Other initiatives support

Table 1. Different possible types of crop rotations during a 3 year period: summer–summer–summer (Rsss), winter–winter–winter (Rwww), summer–winter–summer (Rsws), and winter–summer–winter (Rwsw). In this example, the summer and winter crop periods are represented by black and grey, respectively. The period and duration of the vegetation cycles are estimated according to the approximate seeding and harvest dates of each crop over central and western Europe. Green boxes show favourable periods for the introduction of cover crops that have been considered in this study. Note that this period and its duration vary spatially in Europe.

	YEAR 1												YEAR 2												YEAR 3											
	J	F	M	A	M	J	J	A	S	O	N	D	J	F	M	A	M	J	J	A	S	O	N	D	J	F	M	A	M	J	J	A	S	O	N	D
Rsss																																				
Rwww																																				
Rsws																																				
Rwsw																																				

deforestation or forestation strategies to induce surface albedo changes (Betts 2000, Davin *et al* 2014, Singarayer and Davies-Barnard 2012). An advantage of modifying the continental surface albedo for climate mitigation purposes (Lenton and Vaughan 2009) is that its progressive implementation could help limit the risk of an excessively rapid or strong negative climatic response and could, therefore, be reversed.

This study analyses the radiative forcing changes induced by an increase in the surface albedo of croplands in Europe following the introduction of a cover crop during the fallow period, that is, between the harvest of winter crops and the seeding of the following summer crops. After the harvest, croplands are often bare soil, which has usually a lower albedo than vegetation (Aguiar and Page 1999, Campbell and Norman 1998, Davies and Idso 1979, Oke 1987, Carrer *et al* 2014). The seeding of a cover crop (also referred to as a catch crop or green manure crop) during the fallow period, in places where the period is long enough, would permit more solar energy to be returned to space than when the soil remains bare after the harvest and during the entire winter season (Kaye and Quemada 2017). Many types of plants can be used as catch (or cover) crops. The most extensively used are legume (fava bean, clover) and grasses, but there is increasing interest in brassicas (such as rape, mustard, and forage radish). Another potential advantage of this practice is that it may allow the significant storage of carbon in the form of organic matter in the ground (Justes *et al* 2012, Poeplau and Don 2015), thus combining SRM and CDR approaches (Smith and Rasch 2012), as recommended by the IPCC (2014).

The main objective of this article is to investigate if the inclusion of cover crops in crop rotation is beneficial for climate mitigation purposes and if, therefore, this procedure could be considered by the Europe Commission to counteract climate change in the 28 Member States (EU-28). To this end, we quantify first the potential of global warming compensation resulting from human-induced surface albedo increases due to the introduction of a cover crop at the European scale. In a second part of this work, we also discuss the impact of cover crops on soil carbon sequestration and the use of fertilizer. For this purpose, we use satellite data, land cover databases, meteorological data from model reanalyses, ground measurements, and national agricultural statistics. The potential of these cover crops to increase latent heat fluxes at the expense of sensible heat fluxes, and to decrease surface temperature is not discussed here, even if these processes may increase the mitigation effect (Kaye and Quemada 2017).

2. Methods and materials

2.1. Approach to cover crop inclusion

This section identifies the areas in Europe where cover crops could be sown during the fallow period. Only agricultural areas with annual cropping are included in this study (section 2.1.1). Furthermore, the favourable periods for the introduction of cover crops are not the same everywhere (section 2.1.2).

2.1.1. Location of potential areas for the inclusion of cover crops

Suitable areas are those containing croplands with annual cropping. This includes the two families of arable crops that are predominant in central and southern Europe, summer crops (sown in spring and harvested in autumn) and winter crops (sown in autumn and harvested in early summer). Table 1 presents the four main crop rotations that exist. As the table shows, the duration of the fallow period can either be too short (Rwww, winter–winter–winter case) or be associated with a late and unfavourable seeding period for cover crops (Rsss, summer-summer-summer case). Consequently, cover crops are mainly implanted between a winter crop (after) and a summer crop (before) in Europe (see green boxes, table 1); thus, Rsws (summer-winter-summer case) and Rwsw (winter-summer-winter case) were the only cases considered in this study to quantify the mitigation potential of cover crops.

To estimate the location of croplands in Europe from year to year at a fine spatial resolution, as well as their associated crop rotation type, we used ECOCLIMAP land cover (Masson *et al* 2003, Faroux *et al* 2013) and the European agricultural statistics (Eurostat) in 2011 (http://ec.europa.eu/eurostat/web/agriculture/data/database; last consulted: June 2016). ECOCLIMAP includes 520 ecosystems, or cover types, that are defined at a spatial resolution of 1 km. The heterogeneity of an ECOCLIMAP grid cell includes the mixing of 11 co-existing vegetation types, which may include winter and summer crops. Since ECOCLIMAP does not provide information about the possible crop rotations, the percentages of summer and winter crops and the crop rotation ratios (Rsws, Rwsw, Rsss, Rwww) in the sub-pixels were refined based on agronomical expertise and the 2011 national statistics from Eurostat. By doing this, the correct proportions of winter and summer crops were obtained for each country. Finally, we determined that the winter–summer crop rotation was the most common crop rotation in Europe (26% of the crop rotations).

2.1.2. Period in which a cover crop can be grown

This study analysed data from three years, from 2008–2010, during which the introduction of cover crops in the fallow period was considered. To identify the winter and summer crop harvest and sowing times for each grid cell, we used a method proposed by Gibelin *et al* (2006) and Szczypta *et al* (2012) based on the vegetation index obtained from the ECOCLIMAP database. First, the harvest was estimated to occur in the declining phase of the vegetation index, when it decreases below 40% of the yearly maximum. Second, seeding was estimated to occur when the vegetation index begins to increase the following year. We used the ECOCLIMAP vegetation cycle climatology derived from satellite observations (Faroux *et al* 2013) to estimate these two occurrence dates for the winter and summer crops in each grid cell. For areas where winter to summer crop rotation occurs (mostly in central and southern Europe), the estimated fallow period between the winter crop harvest and the summer crop seeding was considered to be the potential period for the cover crop introduction.

2.2. Radiative forcing

2.2.1. Relationship between surface albedo and TOA radiative forcing

In the remote sensing of continental surfaces, the total surface albedo of a given area (or a pixel, in our case) throughout a full year can be expressed daily as the weighted sum of the vegetation albedo (crop, in our case) and bare soil albedo:

$$\begin{aligned}\alpha(d) &= (1-\mathrm{veg}(d))\alpha_{bs}(d) + veg(d)\alpha_{\mathrm{veg}}(d)\\ \alpha_{\mathrm{CI}}(d) &= (1-\mathrm{veg}(d)-\mathrm{veg}_{\mathrm{CI}}(d))\alpha_{bs}(d)\\ &+\mathrm{veg}(d)\alpha_{\mathrm{veg}}(d)+\mathrm{veg}_{\mathrm{CI}}(d)\alpha_{\mathrm{vegCI}}(d),\end{aligned} \tag{1}$$

where α, α_{bs}, and α_{veg} are the total, bare soil, and vegetation (summer or winter crop here) albedos, respectively. The parameter veg is the vegetation fraction. If a cover crop is added in the crop rotation, a vegetation fraction ($\mathrm{veg}_{\mathrm{CI}}$) of the cover crop is added to the equation (see the second line of equation 1), and the total albedo (α) becomes α_{CI}. α_{vegCI} is the vegetation albedo of the cover crop. Calculations for total albedo are done on a daily basis (d).

The direct radiative forcing in W.m^{-2} at the top-of-atmosphere (TOA) level due to the change in the surface albedo ($\mathrm{RF}_{\Delta\alpha}$), here caused by the introduction of a cover crop in the crop rotation, is expressed in units of time for each pixel, as follows (Lenton and Vaughan 2009):

$$\begin{aligned}\mathrm{RF}_{\Delta\alpha}(\mathrm{W.m}^{-2}) &= -1/\mathrm{Ndays}\sum_{d=1,\mathrm{Ndays}}\mathrm{SW}_{\mathrm{in}}(d)\\ &\times T_a(d)\times\Delta\alpha(d)\\ &\text{with } \Delta\alpha(d)=\mathrm{CI\_Ratio}\times(\alpha_{\mathrm{CI}}(d)-\alpha(d)),\end{aligned} \tag{2}$$

where $\mathrm{SW}_{\mathrm{in}}$ is the total incoming solar radiation at the surface, T_{a} is the upward atmospheric transmittance, $\Delta\alpha$ is the variation in surface albedo, and CI_Ratio is the percentage of cover crop introduction in the Rsws or Rwsw rotation. It is fixed between 0 and the maximum value of the crop rotation ratio (Rsws or Rwsw) in the sub-pixels (according the favourable periods and areas defined in sections 2.2.1 and 2.2.2). $\mathrm{RF}_{\Delta\alpha}$ is the annual average of the daily radiative forcing (d from 1 to Ndays, where Ndays is equal to 1095 in this study, i.e. 3 entire years). The value of the $\mathrm{RF}_{\Delta\alpha}$ at the TOA level is representative of the daily local power in W.m^{-2} that would be reflected back to space due to the introduction of a cover crop. The estimation of $\mathrm{RF}_{\Delta\alpha}$ resulted from 3 years of data, from 2008–2010, and was calculated based on the daily values of radiative forcing. As a matter of fact, all parameters (the albedo values, the vegetation fractions, the incoming solar radiation, etc.) in equation 2 were considered on the daily basis. This means the direct $\mathrm{RF}_{\Delta\alpha}$ over 3 years was calculated for each pixel grid over Europe. The methods for obtaining all the parameters in equation 2 are described in the following section.

2.2.2. The α_{bs}, α_{veg}, and veg data

In the last decade, surface albedo estimates have become available at the global scale using satellite observations from different instruments (Qu *et al* 2015). These instruments allow us to estimate the Earth's surface albedo at a spatial resolution between 500 m and 5 km, with usually less than 10% uncertainty (Carrer *et al* 2010). Given the several types of land covers that co-exist in each satellite pixel at these resolutions, Carrer *et al* (2014) attempted to improve the characterization of the heterogeneity of the grid cells. This was done by developing a mathematical method based on ECOCLIMAP prior information (see section 2.1.1) to derive the surface albedos of up to 11 co-existing vegetation types (grassland, broadleaf, evergreen, summer crop, winter crop, etc.) and a bare soil in the same grid cell. In addition, the method proposed by Carrer *et al* (2014) allowed the effective capture of all seasonal or intra-annual and inter-annual albedo fluctuations of up to 12 pure, co-existing vegetation cover types and their underlying soils in the same pixel grid. The ECOCLIMAP land cover database was here used to determine the fraction of each co-existing vegetation type in a same grid cell. These fractions were readjusted at the country scale with the inventoried fractions of the different crop types provided by the 2011 national statistics from Eurostat (see section 2.1.1). In equation 1, veg, α_{bs}, and α_{veg} were obtained by summing the different contributions from the pure vegetation types (maximum of 12 co-existing types) that exist at the sub-pixel scale. Values corresponding to the pure vegetation characteristics at the sub-pixel scale were from Carrer *et al* (2014). Only the fraction of area covered by the summer or winter crop in a given grid cell was potentially impacted by the introduction of a cover crop in equation 1. In this grid cell, the temporal fluctuations of the bare soil albedo were distinguished from the albedo changes of the different vegetation types. Updates of these values were conducted with the MODIS satellite product (MCD43GF) of the snow-free albedos (bi-hemispherical albedos in the shortwave domain, [0.3–4 μm]) using the Kalman filter method. Again, Carrer *et al* (2014) provided, for the first time, estimates of the temporal evolution of bare soil albedo and vegetation albedos of crops at a global scale (which is necessary to properly conduct this study). These time series from 2008–2010 were used in the present study (albedo data of winter and summer crops and of bare soil - α_{veg} and α_{bs}).

2.2.3. The α_{vegCI} and veg_{CI} data

We interposed the development of some vegetation during the fallow period into the crop rotation between the winter and summer crops (see green boxes in table 1). The fallow period was determined according to the method presented above (see section 2.1). The maximum fractional presence of the cover crop (veg_{CI}) was arbitrarily fixed to 0.95×max(veg). It was assumed here that the level of development (or abundance) of the cover crop will not exceed the maximum level of development of the crop in a given location, a conservative approach. The vegetation fraction of the introduced cover crops gradually increased to the maximum value above. We used a linear interpolation to simulate this increase in the vegetation fraction, corresponding to the growing phase of the crop cover. Then, veg_{CI} remained constant until the cover crop was removed (veg_{CI} set to zero). Different scenarios for the date of removal were tested (see section 2.2.6). Equation 1 was used to estimate each daily value of the crop cover albedo (α_{CI}) derived from the daily estimates of veg_{CI} combined with α_{bs}, and α_{vegCI}. The value of α_{vegCI} was arbitrarily fixed at 0.95×max(α_{veg}), although it could be higher, according to Ferlicoq (2016).

2.2.4. The SW_{in} and T_a data

The incoming solar radiation at the top of the atmosphere (SW_{TOA}) and at the surface level (SW_{in}) reported by the ECMWF (European Center for Medium Range Weather Forecasts) reanalysis (Berrisford *et al* 2011a, Berrisford *et al* 2011b, Dee *et al* 2011) were used in this study. Assuming the upward and downward atmospheric transmittances to be equal, T_a in equation 2 was approximated as the ratio SW_{in}/SW_{TOA}. In comparison, when a mean annual and spatially constant upward T_a of approximately 0.85 is used as in Lenton and Vaughan 2009 and Kaye and Quemada 2017, that value has a tendency to overestimate the $RF_{\Delta\alpha}$. In addition, the rainfall data from this reanalysis was used later in section 3.3 to consider the water needs of the cover crop emergence. Details concerning the satisfactory quality of these ECMWF fields are given in Dee *et al* (2011) and Szczypta *et al* (2012).

2.2.5. Conversion of radiative forcing into equivalent CO_2

Hereafter, we present two methods to convert radiative forcing into equivalent CO_2. The estimations delivered by the two methods will be compared in section 3.

Method 1 (based on a constant CO_2 airborne fraction, AF)—To compare the previously obtained $RF_{\Delta\alpha}$ with sources of CO_2 emissions, Betts (2000), Bird *et al* (2008), Munoz and Campra (2010) and Bright (2015a) convert RF in $W.m^{-2}$ into $kgCO_2$−eq.year^{-1}, as follows

$$RF_{CO_2}(kgCO_2 - eq.year^{-1}) = \frac{S \cdot RF_{\Delta\alpha}}{AF} \times \frac{\ln 2pCO_{2,ref} \cdot M_{CO_2} \cdot m_{air}}{S_{Earth}\Delta F_{2X} M_{air}} \frac{1}{TH}, \quad (3)$$

where S is the area affected by the change in surface albedo (in m^2), $RF_{\Delta\alpha}$ is the radiative forcing at the TOA level (in $W.m^{-2}$; see equation 2), $pCO_{2,ref}$ is a reference partial CO_2 pressure in the atmosphere (383 ppmv), M_{CO_2} is the molecular weight of CO_2 (44.01 g.mol^{-1}), m_{air} is 5.148×10^{15} Mg, S_{Earth} is the area of the Earth (5.1×10^{14} m^2), ΔF_{2X} is the radiative forcing resulting from a doubling of current CO_2 concentration in the atmosphere (+3.7 $W.m^{-2}$), and M_{air} is the molecular weight of dry air (28.95 g.mol^{-1}). With equation 3, the local power in $W.m^{-2}$ due to the albedo change (equation 2) that we estimated at the European spatial scale (surface area S) was converted into global RF_{CO_2} (surface area S_{Earth}). *TH* is the time horizon. Based on the recommendations of Anderson-Teixeira *et al* (2012) and Kaye and Quemada (2017), the time horizon of our potential global warming calculations was fixed at 100 years (which supposes that cover crops will be maintained for this duration during the fallow periods). The per-year CO_2-eq from the albedo change was 1/100th of the total CO_2-eq due to the albedo change. In this way, the estimates of an equivalent CO_2 pulse due to the albedo change can potentially be compared to other sources of CO_2 emissions (for example, the energy, agriculture, or transport sectors). Note that the short analysis times of the cover crop introduction in the crop rotations overemphasize the albedo effect, while long analysis times, such as that in this study, deemphasize this effect (Anderson-Teixeira *et al* 2012). More studies are needed to determine the most appropriate time frame for this analysis;

this is currently an active area of research in environmental biophysics (Bright *et al* 2015b).

Parameter AF is the average CO_2 airborne fraction, defined as the ratio of the annual increase in atmospheric CO_2 to the total CO_2 emissions from anthropogenic sources. In other words, it represents the proportion of human-emitted CO_2 that remains in the atmosphere after a certain period of time. Considering the Bern carbon cycle model (Joos *et al* 2001), after 10 years, 66% of the initial emission remains in the atmosphere due to CO_2 decay over time, while only 36% remains after 100 years. The integral of Bern carbon cycle model gives a 100 year AF value of 0.48 (quite close to 0.5 and 0.55 used by Betts (2000) and Akbari *et al* (2009), respectively). If all variables taking constant values in equation 3 (right-hand term) are grouped into a single parameter ($rf_{CO_2} = 0.908\,W.kg.CO_2{}^{-1}$), we obtain the following, according to Munoz *et al* (2010) and Bright *et al* (2015b):

$$RF_{CO_2}(kgCO_2 - eq.year^{-1}) = \frac{RF(W.m^{-2}) \times S(m^2)}{AF \times rf_{CO_2}(W.kg^{-1}_{CO_2})}\frac{1}{TH}, \quad (4)$$

where *AF* is the atmospheric fraction for a 100 year time horizon (TH=100) and rf_{CO_2} is the derived radiative forcing from 1 kg of CO_2. The uncertainty in these calculations depend on the respective uncertainties of α_{bs}, α_{CI}, SW_{in}, and T_a in equation 2, as well on rf_{CO_2} and AF when RF is converted to $kgCO_2$−eq. For rf_{CO_2}, Akbari *et al* (2009) suggest a ±10% error whereas the error concerning AF is less than ±15% according to Forster *et al* (2007).

Method 2 (Global Warming Potential)—The use of a constant AF does not represent the variations in the emission rates of atmospheric CO_2, which are non-negligible over a 100 year period. The Global Warming Potential method (GWP method, IPCC's emission metrics, Myhre *et al* (2013)), which was also used in this study, attempts to take into account these variations in the atmospheric carbon concentration by using impulse-response functions (IRFs) (Joos *et al* (2013), Myhre *et al* (2013)). The converted CO_2-eq(t) decreases rapidly in the short term but very slowly over the long term. In the same way as above, to obtain a per-year CO_2-eq, we divided the 100 year GWP by 100. Still, as mentioned above, the short analysis times of the cover crop introduction in the crop rotations overemphasize the albedo effect, while long analysis times, like that used in this study, deemphasize this effect.

2.2.6. Scenarios for introducing the cover crops

In the first scenario that we tested, the cover crop was added during the first three months following the harvest of the winter crop, when possible. This three-month period was tested first, as it corresponds to the duration of cover crop introduction period that is recommended in some European countries to limit nitrate pollution when cover crops are used as catch crops. In the second scenario, we accounted for limitations due to the water requirements of cover crops. The rainfall values in each pixel of our study grid were used to limit the area where the crops could grow (figure 2(*c*)). Rainfall data from the ECMWF reanalysis were used with a threshold of 50 mm (the cumulative value for the first month after seeding) for the development of the cover crop. This condition is more restrictive than the requirement of 30 mm, which was estimated by Brisson *et al* (2009). All zones where rainfall is lower than 50 mm were excluded from our calculations in this second scenario. In the third scenario, we calculated the greatest impact by extending the cover crop for a period longer than 3 months, i.e. the longest possible period up to a maximum of 6 months, depending on the duration of the fallow period for each pixel. No limitation due to the water supply was introduced here. In all scenarios, the cover crop was not added if the introduction period was less than 1 month.

3. Results

3.1. Albedo changes

The albedo of bare soil may change with time. In fact, values are usually lower in the winter than in summer due to an increase in the soil water content. Figure 1 shows a comparison between the bare soil albedo values retrieved in August and December 2008. These estimates were derived from MODIS satellite data (Carrer *et al* (2014)). The darkening of soils is one of the most important factors determining how profitable the introduction of the cover crop could be. The areas where the soil was brighter than a given threshold (typically 0.2) in figures 1(*a*) and (*b*) are likely unsuitable for introducing any cover crop. Indeed, the albedo of crops is typically between 0.15 and 0.3, except for some areas, such as Spain, that show a higher bare soil albedo in the summer. Figure 1(*c*) shows the different types of soil classified by the Harmonized World Soil Database (HWSD—Version 1.21; Fischer *et al* (2008)). The darkest soil in the world is the chernozem type (in dark blue, figure 1(*c*)). There are two 'chernozem belts' in the world, and the main one is located north of the Black Sea (see figure 1(*b*)). The albedo of chernozem soil becomes very low in this area in December, and during this period, the soil is often bare due to the fallow.

3.2. The fallow period

We estimated the start date of the fallow period for the winter-summer crop rotation following the methodology presented in section 2.1. This occurs across Europe, on average across, on day 241 (August 29). The fallow period occurs earlier in the southwest than in the northeast of Europe (see figure 2(*a*)). The latest fallow periods start in the northern latitude regions (i.e. Norway,

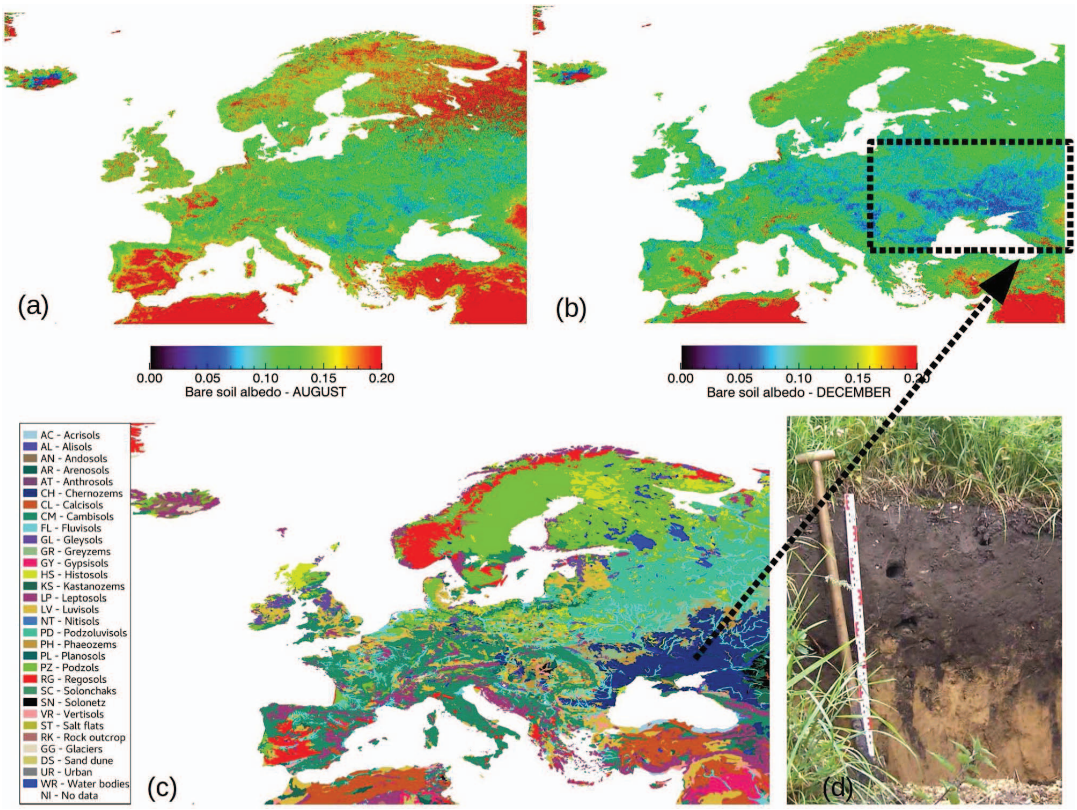

Figure 1. Mean bare soil albedo in August 2008 (*a*) and, December 2008 (*b*) and soil types from the HWSD database (*c*). The black rectangle delimitates the chernozems area (dark blue). A picture of this soil is shown in (*d*).

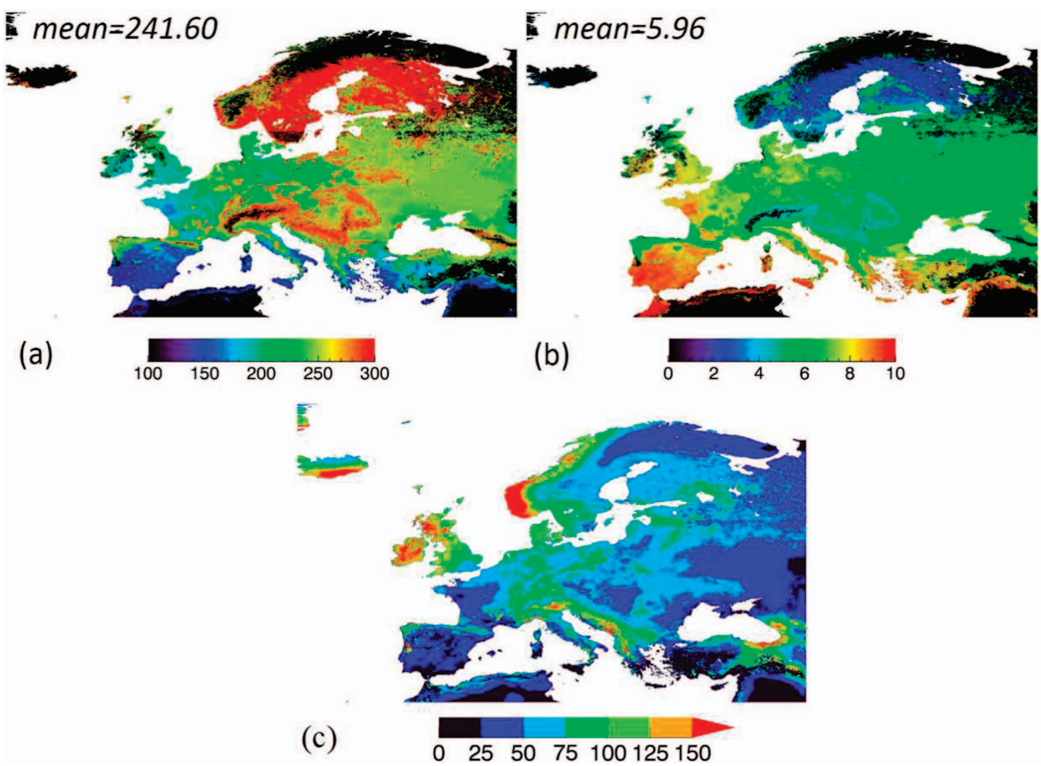

Figure 2. (*a*) Starting date in days after the 1st of January and (*b*) duration in months of the 2008–2009 fallow period for the winter–summer crop rotation (between year 1 and year 2, figure 1 and table 1). (*c*) Mean cumulative precipitation during the month following the starting date of the fallow period (or the seeding of the cover crop) see (*a*).

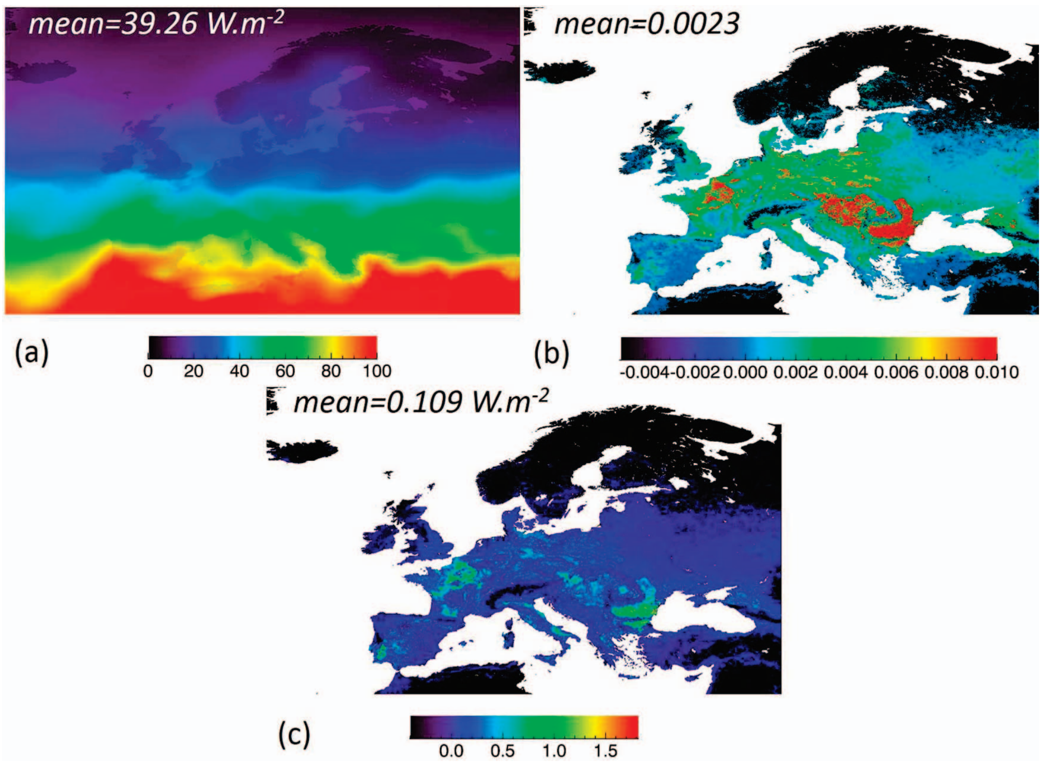

Figure 3. Mean daily value of (*a*) Ta ∗ SW_{in} ($W.m^{-2}$), (*b*) the increase in the surface albedo with the introduction of a cover crop, and (*c*) the radiative forcing ($RF_{\Delta\alpha}$) due to the introduction of a cover crop for the 3 months after the winter crop harvest in 2008 (in $W.m^{-2}$).

Sweden, and Finland) and over mountainous areas (e.g. the Carpathian, Alpes, and Pyrenean Mountains).

Figure 2(*b*) shows the duration of the fallow period between the winter crop and the following summer crop. The average duration of the fallow period is 5.96 months, and it typically varies from 9 months in the southwest (in Spain) to 5 months in the northeast (in the Baltic States) of Europe. Hence, the duration is longer than the 3 months, which corresponds to the first and second tested scenarios (see section 2.2.6), nearly all over Europe, except for in Scandinavia, where it lasts approximately 2 months. It is important to remark that cover crops could be added for periods exceeding 3 months in multiple areas in Europe.

The starting date of the fallow period (figure 2(*c*)) can also correspond to the date of seeding of the cover crop. To discuss the water needs of the cover crop for its emergence, figure 3(*c*) shows the mean cumulative precipitation during the months following the starting date of the fallow period.

3.3. Albedo increase and radiative forcing

The strategy to introduce a cover crop in the crop rotation is described in section 2.1.3. In the first scenario that we tested, the cover crop was added, when possible, during the first three months after the harvest of the winter crop (see figure 2(*a*)). The impact is expressed after averaging the yearly results over three years. The increase in the surface albedo resulting from the introduction of a cover crop ($\alpha_{CI}-\alpha$, equation 2) is shown in figure 3(*b*). The increase in the surface albedo varies geographically and is, on average, equal to 0.0023 over the entire domain during the introduction period. In some places (e.g. France and Romania), the surface albedo of croplands is increased up to 0.15. The magnitude of this increase depends on how dark the soil is (low value of the bare soil albedo, α_{bs}) and how developed the cover crop is (high value of the vegetation fraction of the cover crop, veg_{CI}). In a few places, the bare soil is brighter than the cover crop, thus making the introduction of a cover crop unprofitable (see negative values in figure 3(*b*)). These areas are not discarded from the calculation of the climate change mitigation power. The bare soil albedo has a seasonal cycle, and it usually decreases rapidly after the summer (beginning of the rainy season). During the autumn-winter period, the values of the bare soil albedo across Europe become low (see figures 1(*a*) and (*b*)). The introduction of the cover crop becomes potentially profitable, as can be observed in figure 3(*b*).

Data from the ECMWF reanalysis are used. Figure 3(*a*) shows the mean incoming solar radiation multiplied by the atmospheric transmittance (T_a*SW_{in}, equation 2) during the first three months of the 2008–2009 fallow period (the same period during which the difference in the albedo was calculated in figure 3(*b*)). This number represents the outgoing solar radiation from the Earth in the case of a surface albedo equal to 1. The mean value is 39.26 $W.m^{-2}$, and geographically, it primarily depends on the mean solar

Table 2. Mean average increase in the surface albedo and the associated radiative forcing (in $W.m^{-2}$ and in $MtCO_2$-eq.year^{-1}, respectively) per country for 3 month cover crop introduction period. The percentage of the surface used is indicated relative to the total surface of the country (in %). GHG agricultural emissions are listed in the last column on the right (in $MtCO_2$-eq).

	Surface albedo increase	Albedo-induced radiative forcing	Country area	% use of the country's area for cover crop introduction	Radiative forcing per country (method 1–constant AF)	Radiative forcing per country (method 2–GWP)	Agricultural GHG emissions (2011)
		$W.m^{-2}$	km^2	%	$MtCO_2$-eq.year^{-1}	$MtCO_2$-eq.year^{-1}	$MtCO_2$-eq
Portugal	2.70 E–03	−5.88 E–01	90 608	2.70	7.83 E–02	7.24 E–02	30.09
Italy	1.80 E–03	−2.00 E–01	306 697	3.51	21.62 E–02	20 E–02	30.86
Malta	1.64 E–03	−3.46 E–01	350	3.31	0.02 E–02	0.02 E–02	0.06
Sweden	6.85 E–03	−1.06 E–02	449 857	0.12	0.23 E–02	0.21 E–02	7.17
Finland	1.33 E–03	−1.45 E–02	337 050	0.20	0.29 E–02	0.27 E–02	6.41
Estonia	1.23 E–03	−1.13 E–02	45 285	0.48	0.08 E–02	0.07 E–02	1.22
Latvia	2.27 E–03	−2.33 E–02	65 115	0.98	0.25 E–02	0.23 E–02	2.40
Lithuania	2.14 E–03	−2.34 E–02	65 234	1.96	0.56 E–02	0.52 E–02	4.35
Poland	2.84 E–03	−8.74 E–02	315 623	5.40	15.19 E–02	14.05 E–02	30.09
Czech Republic	2.81 E–03	−1.04 E–01	79 686	5.39	5.21 E–02	4.81 E–02	7.90
Slovakia	5.06 E–03	−1.88 E–01	49 267	7.10	4.83 E–02	4.47 E–02	2.81
Spain	5.42 E–04	−1.04 E–01	507 174	2.99	17.31 E–02	16.01 E–02	34.24
Austria	4.79 E–03	−2.18 E–01	85 066	3.84	4.86 E–02	4.50 E–02	7.15
Hungary	5.36 E–03	−1.71 E–01	94 490	13.09	13.56 E–02	12.54 E–02	5.88
Romania	**6.10 E–03**	**−2.27 E–01**	**243 099**	**10.62**	**36.05 E–02**	**33.34 E–02**	**17.77**
Slovenia	6.14 E–03	−2.35 E–01	20 777	2.72	0.74 E–02	0.68 E–02	1.70
Croatia	4.74 E–03	−1.64 E–01	56 471	4.89	1.85 E–02	1.71 E–02	2.80
Bulgaria	**6.38 E–03**	**−3.73 E–01**	**112 391**	**9.47**	**38.87 E–02**	**35.95 E–02**	**4.90**
Greece	2.80 E–03	−3.09 E–01	136 016	5.30	12.80 E–02	11.84 E–02	8.57
Cyprus	3.41 E–04	−8.05 E–02	9 690	0.52	0.11 E–02	0.10 E-02	0.62
France	**3.30 E–03**	**−2.96 E–01**	**557 639**	**7.87**	**87.38 E–02**	**80.82 E–02**	**77.36**
Ireland	1.31 E–03	−7.03 E–02	70 604	0.81	0.52 E–02	0.48 E–02	17.75
United Kingdom	1.04 E–03	−5.42 E–02	246 934	1.66	5.05 E–02	4.67 E–02	44.01
Belgium	4.38 E–03	−1.58 E–01	30 714	8.90	2.38 E–02	2.20 E–02	10.14
Netherlands	3.04 E–03	−7.03 E–02	37 571	5.08	1.97 E–02	1.82 E–02	18.17
Luxembourg	2.81 E–03	−1.08 E–01	2 721	3.77	0.04 E–02	0.04 E–02	0.66
Germany	**2.81 E–03**	**−1.47 E–01**	**362 390**	**6.20**	**35.14 E–02**	**32.5 E–02**	**64.54**
Denmark	1.22 E–03	−4.49 E–02	43 696	3.97	1.33 E–02	1.23 E–02	10.33
Europe (EU-28)	**2.48 E–03**	**−1.49 E–01**	**4 422 217**	**4.49**	**3.16**	**2.92**	**426.28**

zenithal angle, which explains the south–north gradient. Figure 3(*c*) shows the change in $RF_{\Delta\alpha}$ in $W.m^{-2}$ caused by the introduction of a cover crop after the winter crop harvest in 2008 (the result of a combination of figures 3(*a*) and (*b*), see equation (2). The areas with a strong potential are not always the areas that exhibit the strongest albedo increase (see, for example, southern Portugal in figure 2(*b*)), as high values of atmospheric transmittance and incoming solar radiation are also important. However, the strongest changes in $RF_{\Delta\alpha}$ occur in Romania, Bulgaria, Hungary, Slovenia, and northern France, and these variations are clearly caused by strong albedo increases.

We estimate that the areas where cover crops could be introduced cover 4.17% of the 28 member states of Europe, including 7.87% of France, 9.47% of Bulgaria, 10.62% of Romania, and 6.20% of Germany (see table 2). This area represents 22% of the cultivated crop areas in the EU-28 (34% in France, 30% in Romania, and 21% in Germany). The difference in radiative forcing is lower for high latitude regions where less incoming solar radiation reaches the surface at the time of the cover crop introduction (0.01 $W.m^{-2}$ in Sweden versus 0.59 $W.m^{-2}$ in Portugal on average).

Table 2 also lists the cover crop albedo-induced effect on the radiative forcing per country in the EU-28 converted into $MtCO_2$-eq.year^{-1} by using method 1 (and method 2, see section 2.2.5). France, Bulgaria, Romania, and Germany are the four countries with the greatest mitigation potentials, with changes in RF_{CO_2} of 0.87 (0.81), 0.39 (0.36), 0.36 (0.33) and 0.35 (0.33) $MtCO_2$-eq.year^{-1}, respectively. These values are consistent with the crop yields at the national scale, as France is by far the most important agricultural producer of cereals in Europe, according to Eurostat. The cumulative RF_{CO_2} over EU-28 is 3.16 (2.92) $MtCO_2$-eq.year^{-1}. This value represents 0.74 (0.68)% of the agricultural greenhouse gas (GHG) emissions in 2011, which were equal to 426.28 $MtCO_2$-eq (The Eurostat statistics were updated in 2015, http://ec.europa.eu/eurostat/) (see table 2).

To go further in our study, we tested a second scenario, still based upon a 3 month cover crop development, but accounting for limitations due to the water requirements of cover crops (see section 2.2.6 and figure 2(*c*)). By doing this, we estimated that, for EU-28, the water requirements for the emergence of cover crops could decrease the albedo effect by 28% in the case of no irrigation. The resulting cumulative RF_{CO_2} over EU-28 was 2.27 (2.10) $MtCO_2$-eq.year^{-1}.

Finally, in the third scenario, we calculated the greatest impact of extending the cover crop for a period longer than 3 months, i.e. up to a maximum of 6 months, depending on the duration of the fallow period for each pixel (for that, no water limitation was taken into account). The cumulative RF_{CO_2} over EU-28 was 4.31 (3.99) $MtCO_2$-eq.year^{-1}. With this extension of the cover crop life, we estimated that a compensation level of up to 1.01 (0.93)% of the agricultural GHG emissions could be obtained for the EU-28.

4. Discussion and conclusions

Potential level of climate mitigation. By using MODIS satellite data and the approach developed by Carrer *et al* (2014), we were able to identify areas where the soil is dark enough (low albedo value) to make the introduction of a cover crop profitable. We examined the most likely scenario by introducing cover crops in crop rotations (between the winter and summer crops). We estimated that cover crops could potentially be introduced for 3 months over 4.17% of the surface area of the EU-28. That would represent 22% of the European cultivated surface area. This value at the European spatial scale is quite consistent with the estimate of Poeplau and Don (2015). They estimated that 25% of the global cropland areas (16 million km^2; Siebert *et al* 2010) could potentially be cover cropped.

In Europe, we show that the mean average increase in the surface albedo over these cultivated areas and the associated $RF_{\Delta\alpha}$ of these cover crops are 0.0025 and −0.149 W.m^{-2}, respectively, for the 3 month scenario. If we convert this $RF_{\Delta\alpha}$ into CO_2-eq, it corresponds to a mitigation potential of 3.16 $MtCO_2$-eq.year^{-1}, assuming that the cover-crop practice is maintained for a period of 100 years (2.92 $MtCO_2$-eq.year^{-1}, according to the GWP method). Based on our current knowledge, the estimated uncertainty due to the CO_2 equivalent conversion methodology is approximately 8%. However, it should be remembered that long analysis times, such as that of the current study, deemphasize the $RF_{\Delta\alpha}$ expressed in CO_2 equivalent (Anderson-Teixeira *et al* 2012). Nevertheless, this mitigation potential would represent, every year for a 100 year period, 0.74% of the of the EU-28 agricultural GHG emissions in 2011, which is equal to 426.28 $MtCO_2$-eq. In other words, the introduction of cover crops for 100 years would compensate for 74% of the human-induced GHG agricultural emissions of one year (based on 2011). France, Bulgaria, Romania, and Germany appear to be the four countries with the greatest potential. We show that Bulgaria and Romania have chernozem soil with very low surface albedo in the winter (figure 1). This explains why those two countries are among the countries with the greatest mitigation potentials. The mitigation potential is also probably important for neighbouring countries outside Europe that also have chernozem soil (Moldavia, Ukraine, and Russia, in which the percentage of land used for agriculture is very high).

This mitigation potential of 3.16 $MtCO_2$-eq. year^{-1} is equivalent to a mitigation potential per unit (m^2) of an introduced cover crop over Europe of 15.91 gCO_2.year^{-1}.m^{-2}. We show that this mitigation potential could be increased by 27% if the cover crop is extended for periods longer than 3 months. This magnitude order is consistent with the recent estimations of the albedo effect delivered by (Kaye and Quemada 2017). They showed, using case study sites in central Spain and Pennsylvania (USA), that the surface albedo change due to cover cropping may mitigate 12–46 gCO_2.year^{-1}.m^{-2} over a 100 year time horizon (impact per m^2 of cover crop). Additionally, they estimated that the increase in soil carbon sequestration rates and the decrease in fertilizer due to the adoption of the cover crop practice should mitigate greenhouse gas-based climate change by ∼116 gCO_2.year^{-1}.m^{-2} for non-legumes and by ∼135 gCO_2.year^{-1}.m^{-2} for legumes. This result is consistent with the value of 110 gCO_2.year^{-1}.m^{-2} (per surface unit of cover crop) of the soil C storage effect found by Poeplau and Don (2015). Considering the net biogeochemical effects of cover crops found in Kaye and Quemada (2017) and adding the albedo effect found in this study, the total cover crop mitigation effect would be close to ∼150 gCO_2.year^{-1}.m^{-2}, which would result into a cumulative value over Europe of 29.79 $MtCO_2$-eq.year^{-1} (considering that cover crops could be introduced to 4.17% of the EU-28, as explained below). As the GHG agricultural emissions in 2011 were equal to 426.28 $MtCO_2$-eq., we believe that the introduction of cover crops over Europe may mitigate up to 7% of the human-induced GHG agricultural emissions per year, considering 2011 as the reference year; the impact of the albedo change per year would be between 10% and 13% of this total impact.

Advantages and limitations of cover crop adoption. Little is known about the impact of the introduction of cover crops at a large scale on the climate, even if this practice tends to be imposed on farmers by European legislation for its nitrogen-capture effect. Hence, it is unclear if these changes will generate climate feedback (such as changes in cloudiness resulting from other biogeophysical impacts such as disturbance of roughness or evapotranspiration). According to Ceschia *et al* (2017), the albedo cooling effect of cover crops could be doubled when considering their effect on long-wave radiation. Indeed, in a field scale comparative experiment (cover crop *vs* bare soil), they showed that the dynamic and intensity of the longwave effect was very similar to the albedo-induced cooling effect. Additionally, they found that the radiative cooling effects would be reinforced by a decrease/increase in the sensible/latent heat fluxes at the surface. In another study, Tribouillois *et al* (2018), showed that, compared to bare soil, cover crops increased evapotranspiration (i.e. latent heat fluxes) without limiting the water resources for the next crop, if the cover crop were buried one month before seeding.

Additionally, reducing the area of bare soils by sowing cover crops provides a number of additional ecosystem services (e.g. reductions in soil erosion and nitrogen leaching and increases in biodiversity and soil fertility (Justes *et al* 2012) and probably has an impact on the proliferation of weeds, pests or pathogens. Furthermore, benefits in terms of reducing the use of fertilizers (and associated emissions) should be considered when the cover crops are leguminous. Some disadvantages and limitations to such practices also exist. Although the long fallow period may allow the timing of the cover crop introduction to be adjusted, we showed that the water requirements for the emergence of cover crops could decrease the albedo effect by 28% without irrigation. Furthermore, there is a short-term extra financial cost to farmers associated with cover crop cultivation, as well as small additional GHG emissions caused by seeding and destroying the cover crops (however, these emissions are small compared to the C storage benefits) (Ceschia *et al* 2010). All these feedbacks mechanisms must be carefully evaluated in the upcoming by using climate, economic, and ecological coupled models. From our perspective, a financial compensation for this climate change mitigation service should be encouraged (e.g. via a carbon market). In addition, the cultivation of crops with high water needs should be avoided if it is found that the effect of an additional cover crop would exceed an optimal limit, which still needs to be defined in accordance with equivalent economic criteria. In future work, feedback mechanisms should be analysed to refine the benefits proposed in this study.

Following the COP21. Evidence currently exists that the global warming issue needs to be resolved using attenuation measures and that limitations on GHG emissions are no longer sufficient. Following the COP21 meeting in 2015, the target is to limit global warming below a threshold of 1.5 °C. This new directive, which replaces the previous threshold of 2 °C, has great consequences, as it cannot be achieved even if we were to immediately stop all GHG emissions. Consequently, the resulting outcome of the COP21 is that policymakers will likely need to use geoengineering services for climate mitigation. Using satellite data, this study is in line with other recent studies that estimated the potential mitigation effect of cover cropping. The overall potential of mitigation (resulting from the change in albedo, carbon sequestration, and the change in fertilizer use) could be an appropriate solution (or contribution) that should be encouraged through agricultural policies in the future. As a matter of fact, the introduction of cover crops is in line with the on-going reform of the EU's Common Agricultural Policy, which aims to foster a greening of agricultural surfaces to fight against climate change and for ecological matters. In the upcoming years, the approach presented in this article may, therefore, be weighted against other geoengineering strategies, such as sulfate injections into the atmosphere, according to scientific and ethical criteria.

Acknowledgments

This work was supported by the GHG-Europe (FP7 European grant no. 244122) and Fluxpyr (FEDER Interreg IVa program, ref POCTEFA 08/34) research programs, ADEME (REACCTIF program through the CICC project), Agence de l'Eau Adour-Garonne (BAG'AGES project) CNRS-INSU who is supporting the OSR (Observatoire Spatial Regional), and the Région Midi-Pyrénées Council, and the LSA-SAF project of EUMETSAT. The authors thank the MODIS team who are developing satellite-derived surface albedo products (especially Qingsong Sun and Crystal Schaaf) and the teams that are maintaining the Lamasquère site. The authors also thank J L Roujean, N Boukachaba, E Azzi, C Planque, S Faroux, and R Bright for their assistance.

ORCID iDs

Dominique Carrer https://orcid.org/0000-0003-0117-9973

References

Anderson-Teixeira K J, Snyder P K, Twine T E, Cuadra S V, Costa M H and DeLucia E H 2012 Climate-regulation services of natural and agricultural ecoregions of the Americas *Nat. Clim. Change* **2** 177–81

Aguiar R and Page J 1999 Chapter 3 ESRA Handbook *European Solar Radiation Atlas* ed W Palz, J Greif and J Scharmer 3rd edn (Brussels: Springer)

Akbari H, Menon S and Rosenfeld A 2009 Global cooling: increasing world-wide urban albedos to offset CO_2 *Clim. Change* **94** 275–86

Betts R A 2000 Offset of the potential carbon sink from boreal forestation by decreases in surface albedo *Nature* **408** 6809

Berrisford P, Dee D, Poli P, Brugge R, Fielding K, Fuentes M, Kallberg P, Kobayashi S, Uppala S and Simmons A 2011a *The ERA-Interim archive Version 2.0* (Reading: ECMWF)

Berrisford P, Kållberg P, Kobayashi S, Dee D, Uppala S, Simmons A J, Poli P and Sato H 2011b Atmospheric conservation properties in ERA-Interim *Q. J. R. Meteorol. Soc.* **137** 1381–99

Bird D N *et al* 2008 Incorporating changes in albedo in estimating the climate mitigation benefits of land use change projects *Biogeosci. Discuss. Eur. Geosci. Un.* **5** 151

Bright R M 2015a Metrics for biogeophysical climate forcings from land use and land cover changes and their inclusion in life cycle assessment: a critical review *Environ. Sci. Technol.* **49** 3291–303

Bright R M, Zhao K, Jackson R B and Cherubini F 2015b Quantifying surface albedo and other direct biogeophysical climate forcings of forestry activities *Glob. Change Biol.* **21** 3246–66

Brisson N, Launay M, Mary B and Beaudoin N 2009 *Conceptual Basis, Formalisations and Parametrization of the Stics Crop Model* (Versailles: Edition QUAE) pp 1–1543

Carrer D, Roujean J L and Meurey C 2010 Comparing operational MSG/SEVIRI land surface albedo products from land SAF with ground measurements and MODIS *IEEE Trans. Geosci. Remote Sens.* **48** 1714–28

Carrer D, Meurey C, Ceamanos X, Roujean J-L, Calvet J-C and Liu S 2014 Dynamic mapping of snow-free vegetation and bare soil albedos at global 1 km scale from 10 year analysis of MODIS satellite products *Remote Sens. Environ.* **140** 420–32

Campbell G S and Norman J M 1998 *An Introduction to Environmental Biophysics* 2nd edn (New York: Springer)

Ceschia E *et al* 2010 Management effects on net ecosystem carbon and GHG budgets at European crop sites *Agric. Ecosyst. Environ.* **139** 363–83

Ceschia E, Mary B, Ferlicoq M, Pique G, Carrer D, Dejoux J F and Dedieu G 2017 Potentiel d'atténuation des changements climatiques par les couverts intermédiaires *Innov. Agron.* **62-4** 43–58

Davies J A and Idso S B 1979 Estimating the surface radiation balance and its components *Modifications of the Aerial Environment of Crops* ed B J Barfield and J F Gerber (MO: ASAE St. Joseph) pp 183–210

Davin E L, Seneviratne S I, Ciais P, Olioso A and Wang T 2014 Preferential cooling of hot extremes from cropland albedo management *Proc. Natl Acad. Sci.* **111** 9757–9761

Dee D P *et al* 2011 The ERA-Interim reanalysis: configuration and performance of the data assimilation system *Q. J. R. Meteorol. Soc.* **137** 553–97

Eurostat 2014 Agriculture, forestry and fishery statistics 2014 edn (Luxembourg: Eurostat)

Faroux S, Kaptué Tchuenté A T, Roujean J-L, Masson V, Martin E and Le Moigne P 2013 ECOCLIMAP-II/Europe: a twofold database of ecosystems and surface parameters at 1 km resolution based on satellite information for use in land surface, meteorological and climate models *Geosci. Model Dev.* **6** 563–82

Ferlicoq M 2016 *Comparaison pour les agroécosystèmes des contributions biogéochimiques et biophysiques au forçage radiatif net pour l'identification de leviers d'atténuation au changement climatique* (Université Paul Sabatier) p 353 (http://www.cesbio.ups-tlse.fr/data_all/theses/Th_Ferlicoq_2016.pdf)

Fischer G, Nachtergaele F, Prieler S, van Velthuizen H T, Verelst L and Wiberg D 2008 *Global Agro-ecological Zones Assessment for Agriculture (GAEZ 2008)* (Laxenburg, Rome: IIASA and FAO)

Forster P, Ramaswamy V, Artaxo P, Berntsen T, Betts R, Fahey D W and Nganga J 2007 Changes in atmospheric constituents and in radiative forcing. Chapter 2 *Climate Change 2007. The Physical Science Basis*

Gibelin A, Calvet J, Roujean J, Jarlan L and Los S O 2006 Ability of the land surface model ISBA-A-gs to simulate leaf area index at the global scale: comparison with satellites products *J. Geophys. Res.: Atmos.* **111** D18

IPCC 2014 Climate Change 2014 Summary chapter for Policymakers *Synthesis Report*

Jacobson M and Ten Hoeve J 2012 Effects of urban surfaces and white roofs on global and regional climate *J. Clim.* **25** 1028–44

Joos F, Roth R, Fuglestvedt J S, Peters G P, Enting I G, Bloh W V and Friedrich T 2013 Carbon dioxide and climate impulse response functions for the computation of greenhouse gas metrics: a multi-model analysis *Atmos. Chem. Phys.* **13** 2793–825

Joos F, Prentice I C, Sitch S, Meyer R, Hooss G, Plattner G K and Hasselmann K 2001 Global warming feedbacks on terrestrial carbon uptake under the Intergovernmental Panel on Climate Change (IPCC) emission scenarios *Glob. Biogeochem. Cycles* **15** 891–907

Justes E *et al* 2012 Réduire les fuites de nitrate au moyen de cultures intermédiaires: conséquences sur les bilan d'eau et d'azote, autres services écosystémiques *Rapport d'étude* (France: INRA) p 60

Kaye J P and Quemada M 2017 Using cover crops to mitigate and adapt to climate change: a review *Agron. Sustain. Dev.* **37** 4

Lenton T M and Vaughan N E 2009 The radiative forcing potential of different climate geoengineering options *Atmos. Chem. Phys.* **9** 5539–61

Masson V, Champeaux J L, Chauvin F, Meriguer C and Lacaze R 2003 A global database of land surface parameters at 1 km resolution in meteorological and climate models *J. Clim.* **16** 1261–82

Muñoz I, Campra P and Fernández-Alba A R 2010 Including CO_2-emission equivalence of changes in land surface albedo in life cycle assessment. Methodology and case study on greenhouse agriculture *Int. J. Life Cycle Ass.* **15** 672–81

Myhre G, Shindell D, Bréon F M, Collins W, Fuglestvedt J, Huang J and Nakajima T 2013 Anthropogenic and natural radiative forcing *Clim. Change* **423** 658–740

Oke T R 1987 *Boundary Layer Climates* (New York: Routledge)

Poeplau C and Don A 2015 Carbon sequestration in agricultural soils via cultivation of cover crops—A meta-analysis *Agric. Ecosyst. Environ.* **200** 33–41

Qu Y, Liang S, Liu Q, He T, Liu S and Li X 2015 Mapping surface broadband albedo from satellite observations: a review of literatures on algorithms and products *Remote Sens.* **7** 990–1020

Robock A, Marquardt A B, Kravitz B and Stenchikov G 2009 The benefits, risks, and costs of stratospheric geoengineering *Geophys. Res. Lett.* **36** L19703

Siebert S, Portmann F T and Döll P 2010 Global patterns of cropland use intensity *Remote Sens.* **2** 1625–43

Singarayer J S and Davies-Barnard T 2012 Regional climate change mitigation with crops: context and assessment *Phil. Trans. R Soc. A Math. Phys. Eng. Sci.* **370** 4301–16

Smith S J and Rasch P J 2012 The long-term policy context for solar radiation management *Clim. Change* **121** 487–97

Szczypta C, Decharme B, Carrer D, Calvet J-C, Lafont S and Faroux S 2012 Impact of precipitation and surface biophysical variables on simulated river discharge in Mediterranean Basin *Hydrol. Earth Syst. Sci.* **16** 3351–70

Tribouillois H, Constantin J and Justes E 2018 Cover crops mitigate direct greenhouse gases balance but reduce drainage under climate change scenarios in temperate climate with dry summers *Glob. Change Biol.* (https://doi.org/10.1111/gcb.14091)